Effect of Capacitive Auxiliary Winding on a Three-Phase Induction Motor Performance Behaviour

Mbika Muteba[1], Dan Valentin Nicolae[2]
School of Electrical and Electronic Engineering, University of Johannesburg, Johannesburg, South Africa

***Abstract*—This paper investigates the effect of a capacitive three-phase auxiliary winding on the target variables of a three-phase squirrel cage induction motor (SCIM). The three-phase auxiliary winding is only magnetically coupled to the stator main winding. The three-phase SCIM is modelled using 2D Finite Element Method (FEM). The flux density distribution is numerically computed through the magnetostactic solver, and the other target variables of interst such as the efficiency, power factor and torque are obtained through ac magnetic-transient solver. A conventional 4 kW, 50-Hz, and 4-pole three-phase SCIM is modified to accommodate both main and auxiliary windings in the stator slots. The results obtained from Finite Element Analysis (FEA) are compared with results from experimental measurement. From both simulation and experimental results, it is noted that the capacitive auxiliary winding has not only enhanced the power factor, but it also has a significant impact on the efficiency, torque and other electromagnetic parameters of the three-phase SCIM.**

Keywords—Capacitive auxiliary winding, Efficiency, Power factor, Three-phase induction motor,

I. INTRODUCTION

Three-phase induction motors comprise the vast majority of electric motors made in large sizes. Generally, an induction machine requires reactive power for operation. Thus its power factor is inherently poor, and it is worse especially at starting and when running with light loads. The power factor of an induction machine has been observed to be poor also when operating with power electronics converter. The enhancement of the power factor of induction machine requires a means of reactive power compensation. Several techniques have been suggested for achieving this, which includes the synchronous compensation, fixed capacitors, fixed capacitor with switched inductor, solid-state power factor controller, and switched capacitors [1, 2, 3, 4, 5].

In recent years, the use of an auxiliary winding, which is magnetically coupled to the main winding has been widely proposed in order to address the problems associated with complexity, and ineffective cost of synchronous compensation technique. It meant also to address the issue of voltage regeneration and over voltages, and a very high current inrush during starting in techniques that incorporate directly the connection of capacitors [8, 9, 10, 11]. The use of auxiliary winding is also set to address the problem that techniques that incorporate controlled switches in the stator winding have, which is the generation of large harmonic current in the machine and line. In [8] a static switched capacitor with an auxiliary three-phase stator winding, which is only magnetically coupled to the stator main winding, was explored for improving the starting and operating power factor of a three-phase induction motor. The use of single phase auxiliary winding, which is only magnetically coupled to the stator main winding, and controlled by an active power filter to enhance the power factor of a three-phase induction motor is presented in [10]. In [9] and [11], the injection of leading reactive power into the three-phase (SCIM) to improve the power factor by means of power electronics static switches to control a capacitive single-phase auxiliary winding, is suggested.

As mentioned in above literature, there is a vast number of different techniques that provide reactive compensation of three-phase SCIM through an auxiliary winding. Though, the power factor is proven to be greatly improved for different loading conditions, less analysis has been provided on the effect that reactive compensation has on the other performance variables of interests.

Therefore, this paper analyses the effect that a capacitive auxiliary winding has on the performance indexes of a three-phase SCIM. The target variables of interests analyzed in this paper, include the efficiency, torque, power factor and back electromotive force (EMF).

II. MOTORS SPECICATIONS AND RATINGS

The main and auxiliary windings have the same number of series conductors per phase but with different wire gauge. The auxiliary winding has thinner wire size and high dc resistance than the main winding. The original three-phase SCIM is rated 4 kW. After modification in the stator winding, the rated power is set to be 2 kW for the new motor with three-phase auxiliary winding which is magnetically coupled with the main stator winding. Fig. 1 and Fig. 2 show the stator winding configurations and one pole of the cross section of the three-phase SCIM respectively. Table I depicts the motors specifications and ratings.

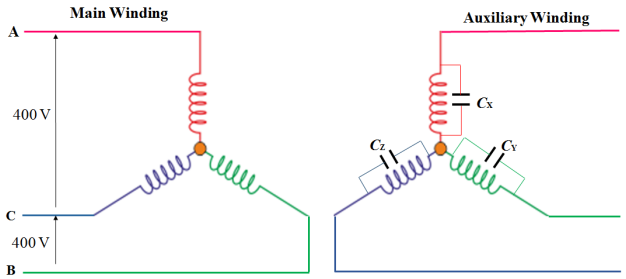

Fig.1. Winding configurations of both main and auxiliary windings.

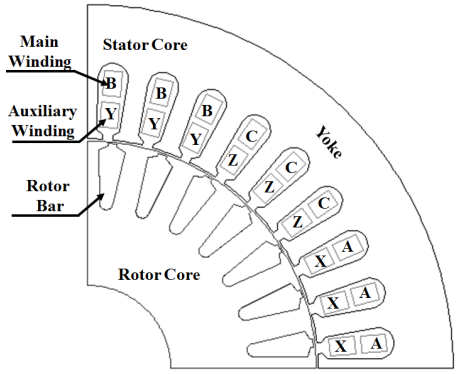

Fig.2. One pole of the cross section of the three-phase SCIM

TABLE I. MOTORS SPECIFICATIONS AND RATINGS

Description	Values
Output power (kW)	2
Rated current (A)	3.75
Rated voltage (V)	400
Rated Frequency (Hz)	50
Rates Speed (RPM)	1427
Number of pole pairs	2
Number of stator slots	36
Number of Rotor Bars	28
Number of turns per phase/Main winding	270
Number of turns per phase/Auxiliary winding	270
Airgap length (*mm*)	0.5
Stator outer diameter (*mm*)	166.4
Stator inner diameter (*mm*)	105.05
Rotor outer diameter (*mm*)	104.05
Shaft diameter (*mm*)	38
Stack length (*mm*)	160.00

III. FINITE ELEMENT ANALYSIS

A. Effect of capacitive auxiliary winding on flux density distribution

In this paper, a two-dimensional (2D) Finite Element Analysis (FEA) is performed using ANSYS 16.0 electromagnetic package. The flux density distribution is computed by using the magnetostatic solver. The phases of the main winding are excited with I_A =3.75 x √2 A, I_B = I_C = -1.875 x √2 A. Due to the symmetry of the motor, only a pole-pitch is considered in the FEA. In Fig. 3 (a), (b) and (c), the flux desity distribution in the iron core is shown for 0 μF, 15 μF and 20 μF capacitive auxiliary winding respectively. Elsewhere in Fig. 4, the radial airgap flux densities and their harmonic contents are illustrated. The airgap flux densities are plotted as a function of rotor position and decomposed into fourier series.

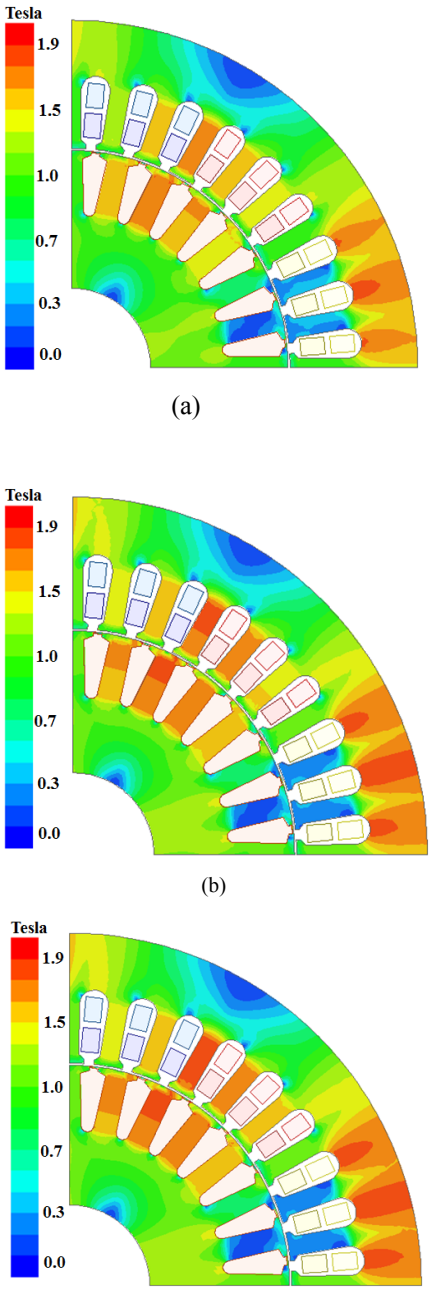

Fig.3. Flux density distribution, (a) Auxiliary winding with 0 μF, (b) Auxiliary winding with 15 μF, (c) Auxiliary winding with 20 μF

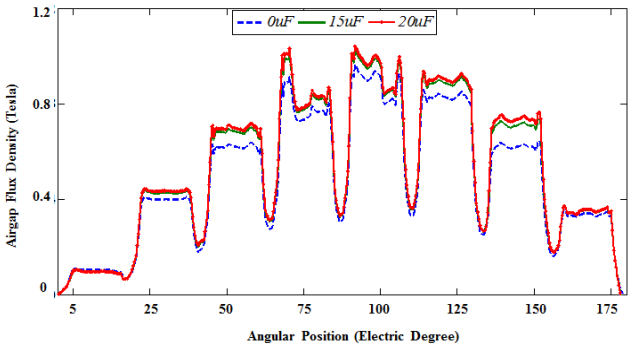

(a)

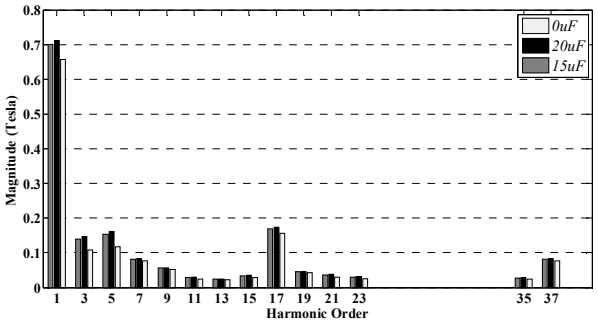

(b)

Fig.4. Airgap flux density, (a) proficles for 0 ,15 and 20 μF , (b) Fast Fourier Transformed

The FEA results in Fig. 3 (a), (b) and (c), show that the magnetic condition of the three-phase SCIM is impacted by the capacitive auxiliary winding. There is an increase of flux density magnitude on the stator back iron and slot tooth when the three-phase auxiliary winding is excited. From Fig. 4, it is evident that with 15 μF and 20 μF capacitive auxiliary winding, the magnitude of the fundamental airgap flux density increases. The increase is also observed for the 3rd and 5th harmonic components of airgap flux density.

B. Effect of capacitive auxiliary winding on line current and back EMF

The ac magnetic-transient solver is used to obtain the current and back EMF in the three-phase SCIM main winding. The FE model has been carried out at rated speed under full-load condition. The full-pitched three-phase main windings are excited by 3-phase sinusoidal voltage. Skin effect and core loss are considered in the FEA. The current and back EMF profiles as function of time are shown in Fig. 5 and Fig. 6 respectively.

Analyzing the FEM results, it is evident that the line current in main winding reduces when an excitation is applied to the three-phase auxiliary winding. With no capacitor connected to the auxiliary winding, the three-phase SCIM draws a RMS line current of 4.34 A. The injection of excitation current by using 15 μF and 20 μF capacitors drops the main winding line current from 4.34 A down to 2.34 A and 1.93 A respectively. The drop of line current contributes to the decrease in stator copper losses. In contrast the RMS induced back EMF increases from 135.67 V, without capacitor to 179.68 V and 195.37 V for 15 μF and 20 μF respectively. The increase in back EMF increases the developed power and torque.

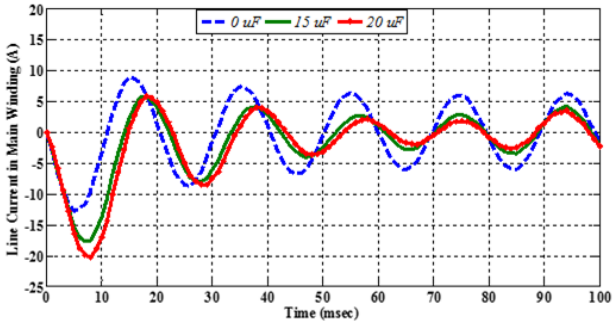

Fig.5. Line current in phase B of the main winding

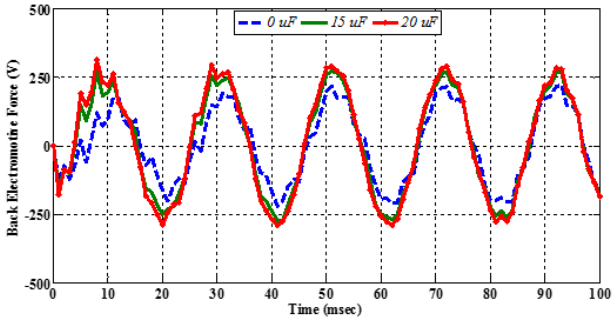

(a)

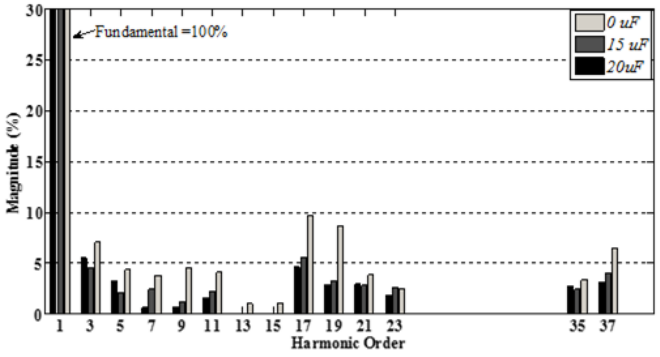

(b)

Fig.6. Induced Back EMF in phase B of the main winding, (a) Profile as function of time, (b) Harmonic components

Observing the harmonic components in Fig.6 (b), it is noted that the back EMF induced in main winding of the three-phase SCIM with no capacitor connected to auxiliary winding has high harmonic components throughout the spectrum. With the injection of excitation current by using 15 μF and 20 μF capacitors, the harmonic components drop tremendously.

C. Motors Equivalent Parameters from FEM

The ideal no-load test is used to determine the magnetizing inductance through Magnetostatic solve. The current is assumed to be zero since the main objective of no-load simulation by finite element is to compute the magnetizing inductance, and to observe the saturation level in different parts of the induction motor. It is noted that only the main winding is excited with magnetizing currents as described previously in sub-section (*B*), and the phase currents are distributed in the stator slot single-layer full-pitched winding. The pitch factor is unity and the winding factor equals to distribution factor.

The fundamental component of the airgap flux-density density is obtained from finite element and for the results are shown in Fig.4. The magnitude of fundamental magnetizing linkage flux is computed analytically using [12]

$$\psi_{m1} = \frac{2}{\pi} k_{w1} N_{ph} \tau_p L_c B_{g1} \tag{1}$$

Where K_{w1} is the fundamental winding factor, N_{ph} is the number of turns in series per phase, τ_p is the pole pitch, L_c is the stator core length and B_{g1} is the magnitude of the fundamental airgap flux density. The main winding phase magnetizing inductance is obtained by dividing the first harmonic linkage flux magnitude to the magnetizing current [12], and it is given by

$$L_m = \frac{\psi_{m1}}{I_m} \tag{2}$$

After computation, the magnetizing inductance and reactance are found to be 0.533 Henry and 167.68 Ω respectively. On the other hand the stator leakage inductance and the rotor resistance are obtained through the locked rotor test. The ac magnetic-transient solver is used at zero speed, and the test is carried out at nearly rated current. The reason of keeping the current to its rated value stems from the fact that the leakage reactance is significantly affected by magnetic saturation. It should be noted that rotor bar skin effect and core loss are considered during in the FEA. The speed been zero, the output mechanical power is zero. Neglecting the iron loss during blocked rotor test, the locked rotor input electrical power P_{LR} is equivalent to total coper loss in the stator winding and rotor bars, and it is directly obtained from finite element. The locked rotor apparent power is computed analytically using

$$S_{LR} = 3V_{LR} I_{LR} \tag{3}$$

Based upon the blocked rotor results, the leakage reactance can be found from the locked rotor reactive power Q_{LR} and it is given by

$$X_L = \frac{Q_{LR}}{3I_{LR}^2} \tag{4}$$

$$\text{Where, } Q_{LR} = \sqrt{S_{LR}^2 - P_{LR}^2} \tag{5}$$

The per phase stator resistance R_s is already known since it is directly related to the number of turns per phase and the cross section of copper wire. The rotor resistance is calculated using

$$R_r = \frac{P_{LR}}{3I_{LR}^2} - R_s \tag{7}$$

The values of stator leakage reactance and rotor resistance are found to be 19.87 Ω and 2.63 Ω respectively.

IV. Practical Results

A. Experimental Set up

The experimental setting comprises of the three-phase SCIM coupled to a Wirbelstrombremse Siemens Eddy Current brake having a maximum load torque of 20 Nm and maximum speed of 3000 RPM. The shaft torque, speed and mechanical power are measured by a rotary type torque transducer with range from 0 to 50 Nm. Fig. 7 shows the experimental setup rig photo.

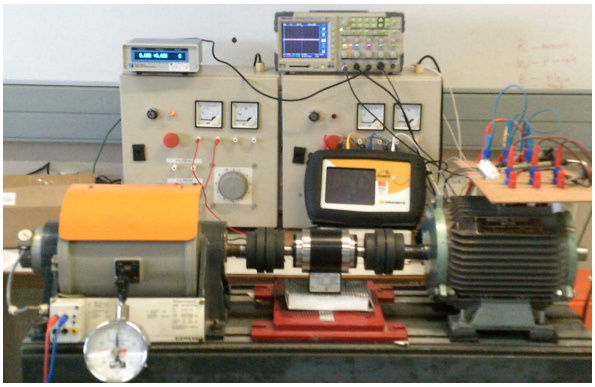

Fig. 7. experimental setup rig photo

B. Induction Motors Equivalent Parameters

The conventional dc, no-load and locked rotor tests are used to determine the parameters of the three-phase SCIM. To determine the magnetizing inductance the machines is fed at rated frequency and rated voltage with eddy current break removed from the shaft. The machine rotates at speed closer to 1500 rpm which is the synchronous speed. The induced rotor current will be small as the speed of the slip is very small. With approximate very small induced current, the stator current is approximately equal to magnetizing current. The rotor resistance and inductance are determined using the locked rotor test, while the stator resistances are determined using the conventional dc test. Table II gives the parameters of the SCIM. The values of magnetizing inductance, stator leakage reactance and rotor resistance obtained from practical measurement are close those values obtained from FEA.

TABLE II. MOTORS PARAMETERS

Description	Values
Stator main winding dc resistance	5.80 Ω
Stator auxiliary winding dc resistance	5.8 Ω
Rotor resistance	3.03 Ω
Equivalent iron losses resistance	949.73 Ω
Magnetizing reactance	180.91 Ω
Stator leakage reactance	16.90 Ω
Rotor leakage reactance	16.90Ω

C. *Performance Analysis*

The performance of the three-phase SCIM is evaluated at full-load for three different auxiliary excitations. Firstly the motor is run with no capacitor connected to the auxiliary winding, and then a 15 μF capacitor is connected followed by a 20 μF. The efficiency, power factor and shaft torque as function of loading are shown in Fig 8, Fig. 9 and Fig. 10 respectively.

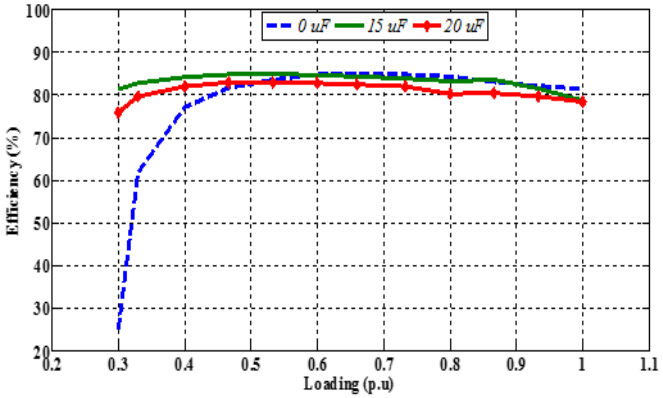

Fig. 8. Efficiency as function of loading.

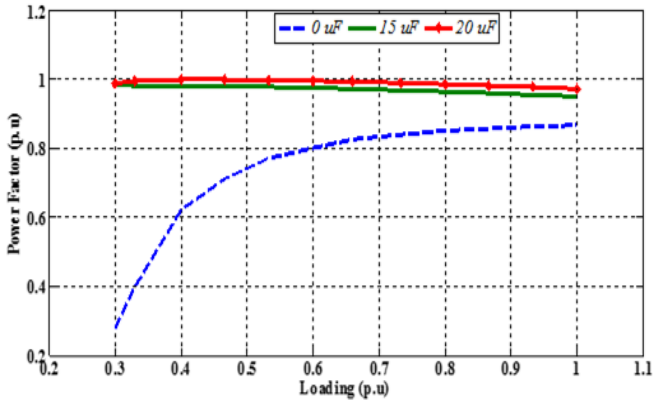

Fig. 9. Power factor as function of mechanical loading

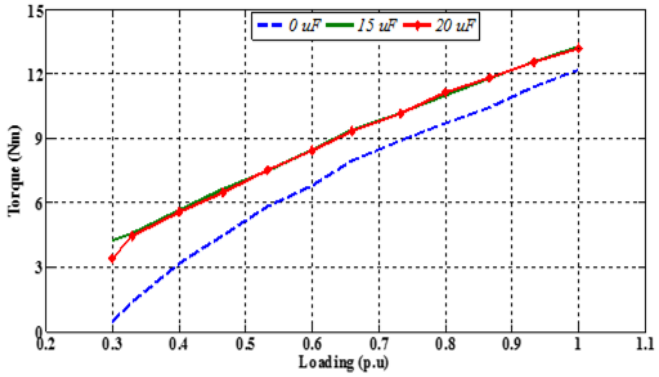

Fig. 10. Shaft torque as function of mechanical loading.

Observing from the experimental results in Fig. 8 , it is clear that the injection of exciation current into the auxiliary winding using either a 15 μF or 20 μF capacitors, improves significantly the power factor from 0.28 to about 0.99 on no-load. The use of 20 μF capacitors gives optimal power factor improvent throughout the loading cycle. The presence of capacitors in the auxiliary winding circuit has also visible effects on the efficiency of the three-phase SCIM as evindenced in Fig. 9. On no-load the efficiency has increased from 25 % (no capacitance injection) to 77 % and 82 % for 15 μF and 20 μF respectively. Under full-load condition, the presence of capacitors do not provide better efficiency as compared to when there are no capacitors connected to the auxiliary winding. The core loss is high when the three-phase SCIM operates with capacitors connected to auxiliary winding. Though the core loss remains constant through the loading cycle, the no-load copper loss during operation without capacitors connected to auxiliary winding is high as compared to operation with capacitors connected to auxiliary winding. This is due to the fact the line current is reduced when the the motor operates with capacitors connected to auxiliary winding. Table III compares the performance indexes experimental and simulation results.

TABLE III. PERFORNACE INDEXES AT FULL-LOAD

Performance Indexes	Capacitance Value					
	0 μF		15 μF		20 μF	
	Exp	Sim	Exp	Sim	Exp	Sim
Efficiency (%)	81.4	82.5	78.8	88.7	78.4	90.8
Power factor (p.u)	0.87	0.86	0.95	0.96	0.97	0.96
Torque (Nm)	12.1	9.2	13.2	12.2	13.4	13.5
Main Current (A)	3.75	4.38	3.5	2.34	3.5	1.93

The three-phase SCIM with capacitors connected to auxiliary winding develops a high power and torque at reduced line current throughout the entire loading cycle. This is due to high fundamental back EMF induced in main winding when operating with capacitive auxiliary winding. Furthermore, Fig. 10 evidenced that the torque is positively impacted by the capacitive auxiliary winding.

V. CONCLUSION

In this paper, the effect of a capacitive auxiliary winding on performance of a three-phase squirrel cage induction motor were analyzed. Reading from both Finite Element Analysis and experimental results, it is clear that the injection of capacitive current into the auxiliary winding had not only improved the motors power factor, but also had influenced the efficiency and the torque. The optimal value of the capacitors should be carefully selected to provide at the same time power factor correction and improved performance of the three-phase squirrel induction motor with capacitive auxiliary winding. As noticed from the analysis, it is possible to have better the power factor, the torque and efficiency through a wide range of loading operation.

REFERENCES

[1] E. Muljadi, T.A. Lipo, and D.W. Novotny, "Power Factor Enhancement of Induction Machines by Means of Solid State Excitation", Research Report 86-3, Wisconsin Electric Machines and Power Electronics Consortium (WEMPEC), May 1986.

[2] Bor-Ren Lin, Chun-Hao Huang and Zheng-Zhang Yang. Three-Phase Power Factor Corrector Based Oncapacitor-Clamped Topology. Proceedings - IEEE International Symposium on Circuits and Systems. pp. 3643 -3646 .2005

[3] N. Bianchi, S. Bolognani, F.Tonel Thermal Analysis of a Run-Capacitor Single-Phase Induction Motor. IEEE Trans Ind Appl. pp. 457-465.2003

[4] T. A Lattemer, D.W Novotny and T. A. Lipo, " Single-Phase Induction Motor with an Electronically Controlled Capacitor", *IEEE Trans. On Industrial Applications,* Vol. 27, No.1, Jan/Feb, 1991, pp. 38-43.

[5] C. Suciu, L. Dafinca, M. Kansara and I. Margineanu, " Switched Capacitor Fuzzy Control for Power Factor Correction in Inductive Circuits," Proceedings of Power Electronics Specialists Conference, Irlanda, June, 2000

[6] Wu Hanguang, Chen XIUMIN, Lu Xianliang and You Linjuan."An Investigation on Three-Phase Capacitor Induction Motor", *Proceedings* of Third Chinese International Conference on Electrical Machines. Aug 29-31, 1999. Xi'an, China, pp 87-90

[7] M. A El-Sharkawi, S. S Venkata, T. J Williams, and N. G Butler," An adaptive Power Factor Controller for Three-Phase Induction Generators", Paper 84 SM 672-2 presented at the IEEE/PES Summer Meating, Seatle, Washington, July 15-20, 1984.

[8] Jimoh Adisa A. Nicolae Dan V. A study of improving the power factor of a three-phase induction motor using a static switched capacitor. 12th International Power Electronics and Motion Control Conference, pp.1088-1093, 2006

[9] A.A. Jimho, D.V. Nicolae, "Controlled Capacitance Injection into a Three-Phase Induction Motor through a Single-Phase Auxiliary Stator Winding" 2007 IEEE Power Electronics Specialists Conference,

[10] M. Muteba, A. A. Jimoh, D. V. Nicolae "Improving Three-Phase Induction Machines Power Factor Using Single Phase Auxiliary Winding Fed by an Active Power Filter", 2007 IEEE African Conference

[11] D.V Nicolae, A. A. Jimoh "A Three-Phase Induction Motor with Power Electronic Controlled Single-Phase Auxiliary Stator Winding", 2007 IEEE International Electric Machines and Drives.

[12] I. Boldea, L. Tutelea, "Electric Machines: Steady State, Transients, and Design with Matlab",CRC Press, Taylor & Francis, 210